

# Characterization of explosively bonded iron and copper plates

Z. LIVNE, A. MUNITZ

*Nuclear Research Centre-Negev, PO Box 9001, 84190, Beer-Sheva, Israel*

Explosive bonding between iron and copper plates was achieved under various conditions. A variety of experimental techniques were applied in order to investigate the bonding interface, including metallography, scanning electron microscopy, X-ray micro-analysis and X-ray diffraction. It was found that the bonding characteristics depend on the ratio of the explosive weight to the flyer plate weight ( $R$  ratio) and on the distance ( $X$ ) from the detonation point. The microstructure of the molten pockets obtained depends strongly on their composition and on the cooling rate. Increasing the copper content in the molten pocket and the cooling rate resulted in a finer structure. Microstructural similarities between electron-beam molten surfaces and molten pockets in explosively bonded plates indicate, that cooling rates as high as  $10^5$  K  $\text{sec}^{-1}$  are obtained in both cases.

## 1. Introduction

Explosive bonding of metals is known to be capable of producing large area bonding between metal plates, including couples of grossly different mechanical properties. A well-known example is the bonding between large plates of lead and steel, which cannot be achieved by any other means [1]. A typical industrial application of explosive bonding is the welding of pipelines for heat exchangers [2].

The technological development of metal bonding by explosives started in the 1940s. The progress made since then is reviewed in several papers [1, 2]. A detailed description of the process is given by Bahrani *et al.* [3]. Briefly, a flyer plate is supported with minimum force parallel or at an oblique angle, to a parent plate. The flyer plate is covered by a buffer, which may be made of a thin rubber sheet. The explosive is then placed on top of the buffer sheet, and is detonated by an electric detonator, placed along the lower plate edge [3]. Following the explosion, the flyer plate collapses on to the parent plate, and a metallic jet is formed at the impingement line between the two plates. A complete metallic bond, which is usually wavy, appears between the two plates. Most of the investigators considered the formation of the metallic jet as the most important mechanism in the explosive bonding process. The back-and-forth jet motion during the explosion-front propagation was regarded as the cause of the bonding-wave formation. The size and shape of the waves varies with bonding parameters. It was noticed that each wave consists of a front vortex and a rear vortex [3, 4] (see Fig. 1). It is believed that the vortices are created by the entrapment of the metallic jet between the bonded plates. This trapping causes the creation of high local temperatures at the centre of each vortex, which could cause melting and subsequent solidification. Such molten zones, will henceforth be referred to as "molten

pockets". Their study should provide a means for a better understanding of explosive bonding processes.

The solidification characteristics at molten pockets depend on the interaction between the elements constituting the bonded couple. We classify the possible interactions into three categories:

(a) complete miscibility between the two elements. The mechanical strength of molten pockets created under such conditions are comparable or even higher than that of the weaker component of the couple;

(b) formation of intermetallic compounds, which are generally very brittle. The mechanical strength of the pockets thus created, is very much degraded compared to the mechanical strength of each component separately;

(c) very low mutual miscibility. The influence of such low miscibility on the mechanical properties of the bonding has not yet been clarified.

Iron and copper are two metals which have very low mutual miscibility, and do not form intermetallic compounds. The objective of the present research was to get a better insight into the solidification characteristics of molten pockets in the bonding zone of iron and copper plates, and their influence on the mechanical properties of the bond.

## 2. Experimental details

In the present study we have used copper and iron plates of dimensions  $200 \times 300 \text{ mm}^2$  as the flyer and parent plates, respectively. The explosive material was TNT +  $\text{NH}_4\text{NO}_3$ , which has a detonation velocity of  $2200 \text{ m sec}^{-1}$ . We have performed bonding between the copper and iron plates using various conditions, such as parallel plates, oblique plates, and different ratios between explosive weight and the flyer plate weight ( $R$  ratios). After bonding, the joined plates were cut in different directions. The strength, hardness,

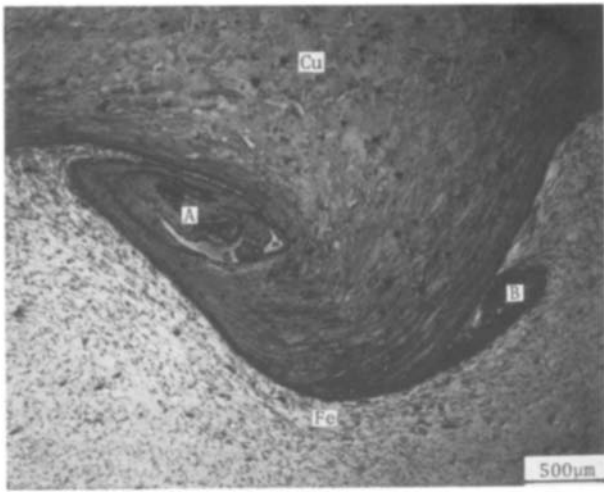


Figure 1 A wavy interface in a Fe–Cu bond demonstrating front (A) and rear (B) molten pockets.

composition, and metallography were studied for each pair of bonded plates.

The bonded plates together are too thin (only 6 to 20 mm) to allow the extraction of a standard tensile specimen for tensile strength studies. There was also no point in applying the standard shear test as it could not properly represent a case of a wavy bond such as in our case. Therefore, a special device (Fig. 2) was used in order to evaluate the bonding mechanical properties. Samples for tensile strength tests were prepared as follows: a circular plate of diameter 28 mm was drilled out of the large plate, with a drilling cup. The diameter of the copper side was then reduced to 14.5 mm, and a hole of 11.5 mm diameter was drilled in the centre of the iron plate up to the Cu/Fe interface. The sample was placed on a specimen holder, and a pushing rod was inserted into the hole, touching the iron plate. Then, the pushing rod was pressed down until the sample ruptured. The rupture stress was calculated from the pressing force, and the circular cross-sectional area upon which it acted. The morphology of the ruptured area was examined with a scanning electron microscope (SEM).

Specimens for metallography, microstructure and

micro-analysis were cut in the form of rectangles, which included the bonding interface (Fig. 3). We usually inspected areas on plane A which included the bonding interface and the molten pockets. In some cases, the copper top part (plane B in Fig. 3) was abraded to reveal the molten pockets. Each surface was mechanically polished with diamond paste, with a final stage of  $0.25\ \mu\text{m}$ . This procedure was sufficient for microprobe examination. The microstructure analysis was carried out using an electron microprobe (JXA5 Jeol), operating by an X-ray wavelength detection method. Constitutional variations along various lines were made across each of the molten pockets studied, thus revealing the average composition of the different molten pockets. For scanning electron microscopy (Philips type 505 SEM with EDAX accessory), and for metallography, the specimens were etched further with either of the following etchants: (I) 2 ml  $\text{HNO}_3$  in 100 ml methanol (“Nital”), operating at room temperature, for 5 sec; (II) 2 g  $\text{FeCl}_3$  + 10 ml  $\text{HCl}$  in 95 ml ethanol, operating at room temperature, for 10 sec. The first one is an efficient iron etchant, and is used to expose the microstructure of iron-rich zones. The second one is an efficient copper etchant, and is used to expose the microstructure of copper-rich zones. Sometimes, both etchants were used in succession, thus revealing more information on the microstructure. Secondary electron images (SEMs) were studied, along with energy dispersive analysis of the emitted X-rays (EDAX). The EDAX was capable of providing compositional analysis of precipitated phases which were larger than about 5 to  $10\ \mu\text{m}$ .

One of the goals of the present study was to compare the microstructure of the molten pockets to that of a conventional Fe–Cu cast. As a standard reference we have used a 10 g mixture of iron with 40 wt % copper. The starting materials were first melted in a ceramic crucible, and then poured over a water-cooled copper plate. Solidification rates were approximately  $10^3\ \text{cm sec}^{-1}$ . Another reference material was created by electron-beam surface melting and subsequent solidification by self quenching. The melting conditions were as follows: driving voltage 60 kV, current 5 to 10 mA, electron-beam scanning velocity  $\sim 500\ \text{cm}$

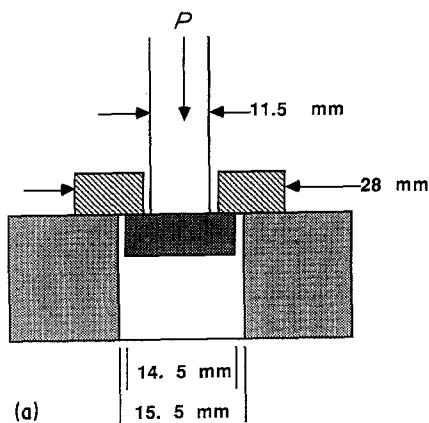


Figure 2 The special device for measuring the mechanical properties of the bonded plates: (a) schematic drawing; (b) general view.

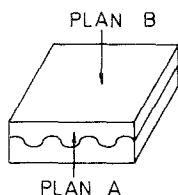


Figure 3 Schematic illustration of sample geometry. The inspection planes are marked on the figure.

$\text{min}^{-1}$ . The electron beam focus was about 1 mm beneath the molten surface. Cooling rates as high as  $10^5 \text{ K sec}^{-1}$  were achieved [5, 6].

### 3. Results and discussion

#### 3.1. Cast Cu–Fe microstructure

In Fig. 4 we show secondary electron images (SEMs) of Fe–40 wt % Cu alloy quenched on a water-cooled copper plate. The figure reveals a dendritic structure, consisting of primary dendrite arms about  $100 \mu\text{m}$  long and  $10 \mu\text{m}$  wide. Microprobe micro-analysis shows that up to 14 wt % Cu could be dissolved in a dendritic arm (see Fig. 4a). Observation of the Fe–Cu equilibrium phase diagram [7], indicates an upper limit of about 14% miscibility of copper in the  $\gamma$ -Fe phase, and almost negligible miscibility of copper in the  $\alpha$ -Fe phase. In our case primary  $\gamma$ -Fe dendrites, solidify first, they dissolve up to 14 wt % copper. The  $\gamma$ -Fe phase is unstable at room temperature. It transforms into the  $\alpha$ -Fe phase. Indeed, no  $\gamma$ -Fe phase could be detected by X-ray diffraction. All the sample volume contained only  $\alpha$ -Fe or  $\epsilon$ -Cu phases. However, copper is immiscible in  $\alpha$ -Fe. It then precipitates in the dendrite arm, as the primary  $\gamma$ -Fe crystals transform into the  $\alpha$  form. Upon etching with Nital, a fine microstructure is revealed in the primary  $\alpha$ -Fe crystals (see Fig. 4b). The dendrite arms are embedded in a copper-rich matrix (68 wt % Cu). It consists of primary  $\epsilon$ -Cu, as well as  $\alpha$ -Fe secondary phases, which transform from the secondary  $\gamma$ -Fe phase. Precipitated copper is expected to exist inside the  $\alpha$ -Fe, but could not be seen with the present resolution.

#### 3.2. Bonding interface morphology

Usually the explosively bonded Fe–Cu interface is not planar. Very often, a wavy interface is obtained, the

form of which is determined by several parameters, such as the  $R$ -ratio (ratio between the weights of the explosive charge and the flyer plate), the inclination angle between the plates, and the distance from the detonation point [8]. Each wave contains two molten pockets: one is the region where the wave rises, which is referred to as the front location (marked A in Fig. 1). The other one is the region where the wave descends, which is referred to as the rear location (marked B in Fig. 1). Metallographic characterization of the explosively bonded interface may be parameterized by the following:

1. the wavelength of the interface modulation and its amplitude;
2. the morphology and position of the molten pockets along the wave, and
3. the microstructure of each molten pocket.

In one of our experiments, the bonded plates were placed parallel, 1 mm apart, while the  $R$ -ratio was changed in the direction perpendicular to the detonation propagation (Fig. 5). In Fig. 6 we show a series of optical microscope photographs demonstrating the wave morphology as a function of the distance  $X$  from the detonation point for various  $R$  values. It is seen, that both wavelength and amplitude increase for increasing  $R$  values. Also, both wavelength and amplitude are increasing functions of the distance from the detonation point. One can also see that for  $R = 0.85$  and a distance  $X$  smaller than 230 mm, no bonding is achieved. A good bond is created at a distance  $X > 270$  mm. On the other hand, increasing the  $R$  value to 1.15 creates a planar bond already at the detonation point. For  $R = 1.15$  a wavy bond interface is created after about 70 mm from the detonation point, while for  $R > 1.47$  a wavy interface is formed for any distance  $X$ . The thickness of the molten pockets increases with increasing  $R$  and  $X$ .

#### 3.3. Microstructure of the molten pockets

The cooling rates depend on the molten pocket thickness, and vary across the molten pocket cross-section. In the centre of the molten pockets the cooling rates are the lowest, and they increase towards the circumference. Since the microstructure depends on the cooling rates, a variety of microstructures is expected between different pockets, as well as within the

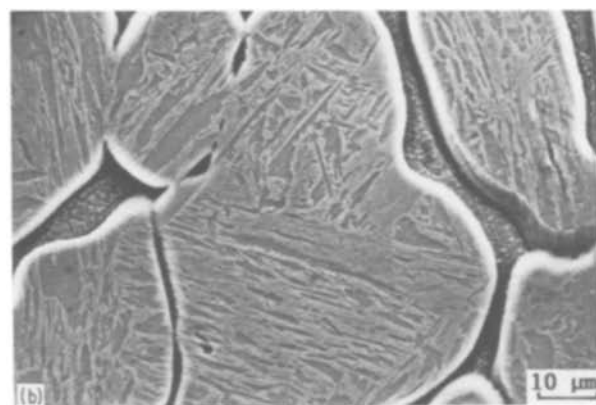
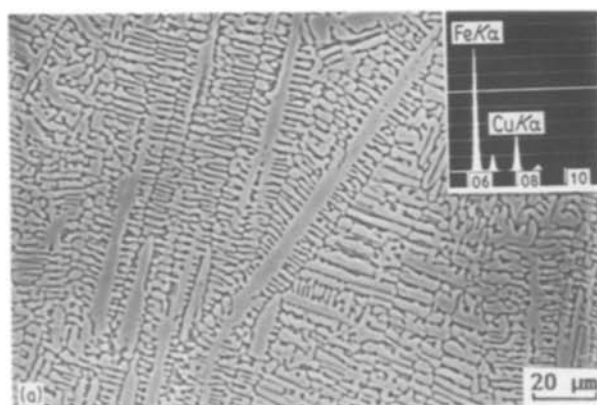


Figure 4 Secondary electron images (SEMs) of Fe–40 wt % Cu quenched on a water-cooled copper plate. (a) General view. A typical X-ray spectrum of dendrite arm is given in the right side. (b) A cross-section of dendrite arm after etching with nital.

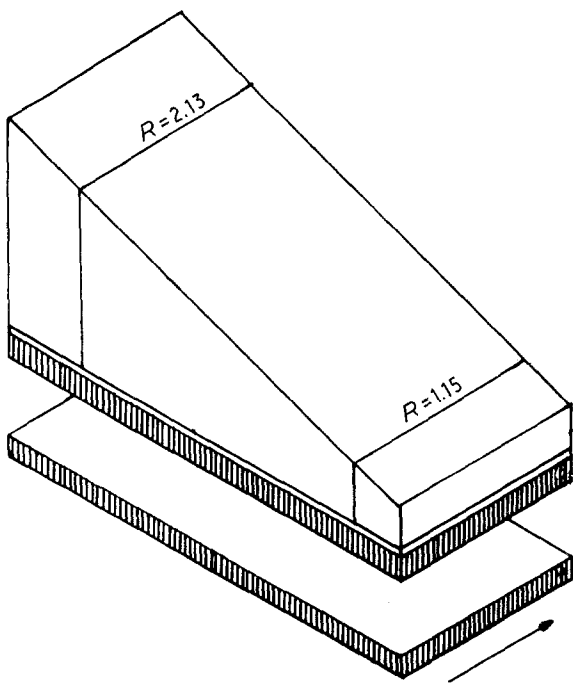


Figure 5 Schematic illustration of the  $R$ -ratio variation perpendicular to the detonation propagation in a special experiment.

pockets themselves. Metallographic examination as well as scanning electron microscopy (SEM) examination, reveal two different types of molten pockets:

1. molten pockets with a fine homogeneous structure (see Fig. 7a);
2. molten pockets which contain large smooth particles of dimensions of the order of 1 to 30  $\mu\text{m}$ , which are embedded in a very fine homogeneous struc-

ture (Fig. 7b). These particles appear smooth for the highest resolution used (10 nm) and for different etching procedures. Compositional micro-analysis examination indicates that these are, in fact, pure iron particles, as shown in detail in the Section 3.4. In Fig. 8 we show a secondary electron image photograph demonstrating the similarity between the microstructure of the molten pockets and that of rapidly resolidified electron-beam molten surfaces (compare Fig. 7a with Fig. 8). The similarities between both microstructures imply that cooling rates as high as  $10^5 \text{ K sec}^{-1}$  could be obtained during resolidification of the molten pockets.

The microstructure of the molten zones varies across the molten pockets. In the centre the structure is coarser, while at the circumference the structure becomes finer. It is likely that this difference is caused by the different cooling rates involved during resolidification of the molten pocket at different locations. It appears that the microstructure depends also on the composition.

### 3.4. Compositional micro-analysis of the molten pockets

We have carried out compositional micro-analysis on a large number of molten pockets. The compositional analysis shows different compositions for different molten pockets. The compositions of various pockets formed at the same bond varied appreciably and these variations are clearly dependent on the experimental conditions and the position in the wave. There is a difference between front pockets, which are usually iron-rich (parent plate material) and rear pockets

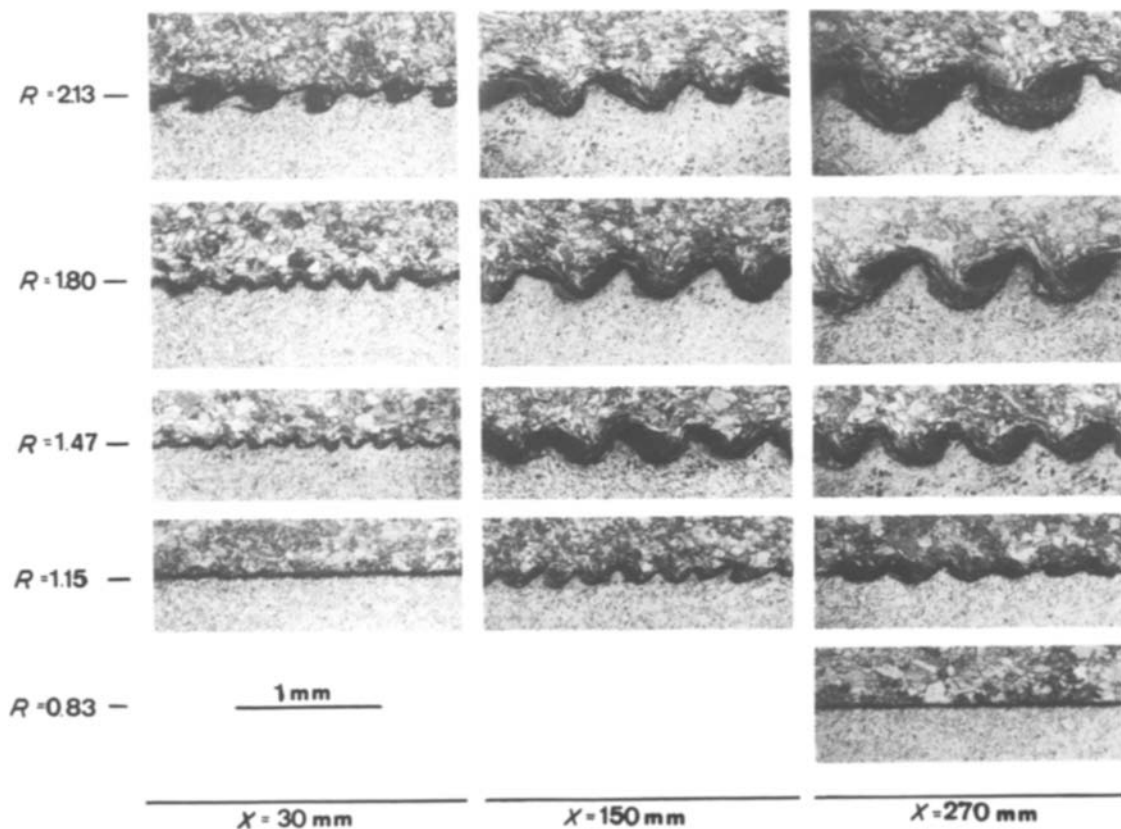


Figure 6 A series of optical microscopy photographs demonstrating the bonding interface characterization as a function of the  $R$ -ratio and the distance from the detonation point.

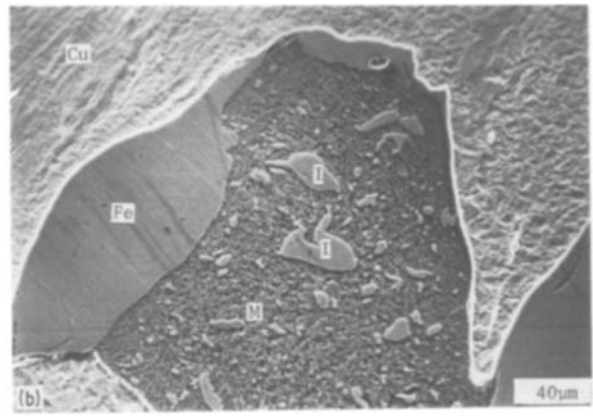
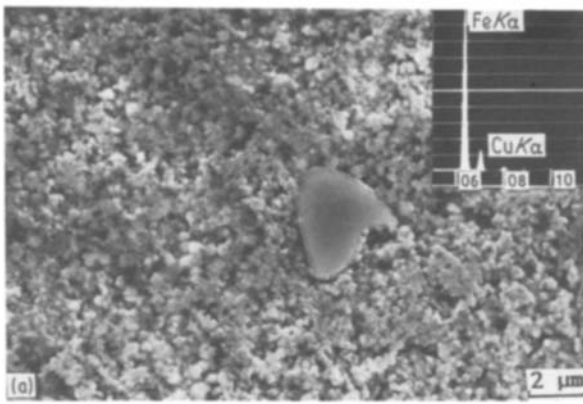


Figure 7 Secondary electron images (SEMs) demonstrating the different kinds of microstructures found in the resolidified molten pockets. (a) Homogeneous structure; (b) iron smooth particles embedded in a homogeneous structure.

which are usually copper-rich (flyer plate material). Also, there are compositional differences between pockets.

In Fig. 9 we show a histogram of the number of pockets as a function of the average composition of the pocket. The results are based on an examination of more than 50 different rear pockets. The figure reveals that a molten pocket contains no more than an average of 88 at % Fe. The arrow in the figure indicates the pocket composition reported by Trueb [9]. We can see that Trueb's results coincide with our most probable composition. The most frequent composition range is between 18 and 45 at % Fe. The composition in the molten pockets depends on the bonding parameters, and on the location of the inspected area in the molten pockets. There are also compositional variations in the pocket itself between the centre and the circumference. Some molten pockets contain smooth particles. X-ray elemental point count for these particles, without interference of signals from the surrounding area, could be made for a particle larger than about 10 μm. The results show that these particles contain more than 99 wt % Fe and less than 0.9 wt % Cu. The copper signal could emanate from copper dissolved in the iron or from the background. Most likely these particles are iron pieces torn away from the iron plate by the large melt convections, a result of the large turbulent flow induced by the high pressure involved in the process. The

particles may have melted, but did not have sufficient time to dissolve homogeneously before resolidification. More probable the remainder of the torn iron particles have not melted at all. The presence of tiny spheres attached to the big particles (see Fig. 7a) indicates that the particle circumference, however, has melted and resolidified.

The microstructure is influenced not only by the solidification rates, but also by the composition. In Fig. 10 we show a series of secondary electron images (SEMs), demonstrating the influence of the molten pocket composition on the resolidified molten pocket microstructure. At a composition of about 40 wt % Cu the microstructure consists of tiny spheres. As the copper concentration increases the microstructure becomes finer. It thus appears that the microstructure depends on both cooling rates and compositions, as found in other systems [6].

### 3.5. Mechanical properties of the explosive bonds

The tensile strength of the Fe–Cu bonded plates was measured according to the procedure described in Section 2. It is found that the tensile strength of the bonded iron and copper plates ranges between 30 and 38 k mm<sup>2</sup>. This tensile strength is at least as high as the copper tensile strength. Indeed, in many experiments,

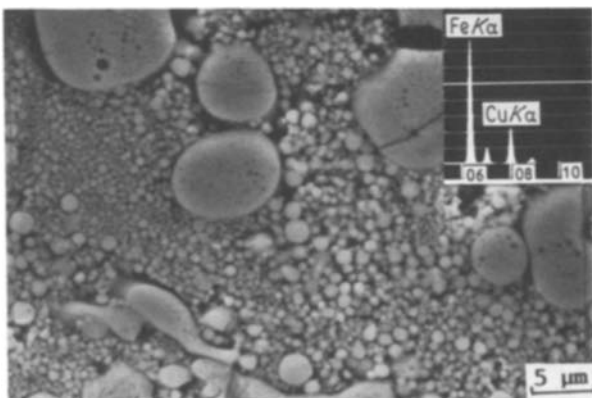


Figure 8 Secondary electron image illustrating the microstructure of a resolidified surface melted via electron beam surface.

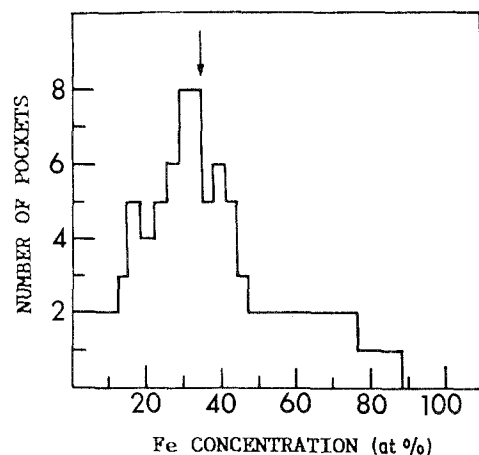


Figure 9 An histogram of the number of molten pockets as a function of the average pocket composition. The arrow indicates the pocket composition reported by Trueb [9].

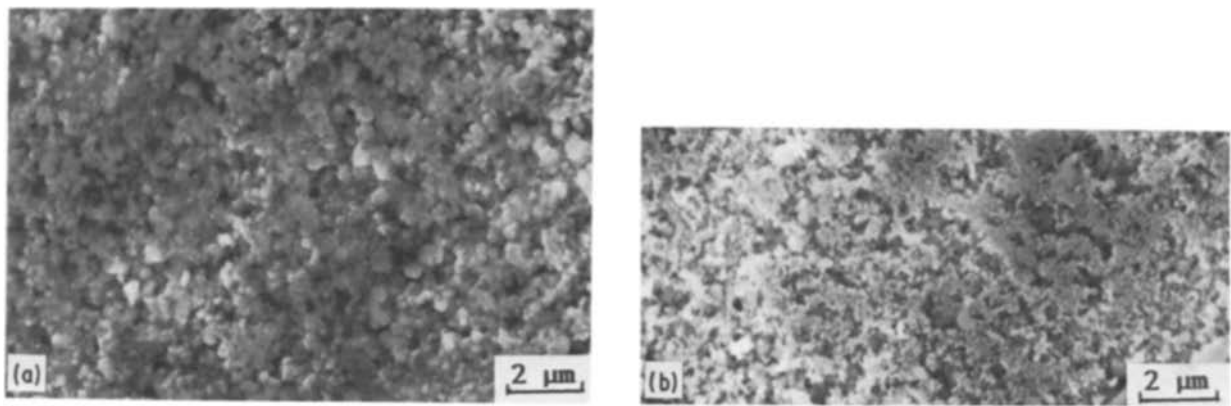


Figure 10 A series of secondary electron images showing the microstructure dependence on compositional variations. (a) 40 wt % Cu; (b) 60 wt % Cu.

the rupture zone does not pass through the molten pockets but in the copper plate side. A typical microstructure of the ruptured zone is given in Fig. 11. The figure reveals a dimples structure, which is characteristic of the ductile copper plate nature. It appears that the tensile strength is independent of the  $R$ -ratio. We attribute the high tensile strength achieved in the Fe–Cu bonded plates to the lack of intermetallic compounds at the interface. In other pairs of bonded plates, such as Al–Cu, a brittle intermetallic compound is formed at the bonded interface and the tensile strength of the bond is degraded.

#### 4. Conclusion

We have successfully created explosive bonding between iron and copper plates under a variety of conditions. It is found that the bonded interface characteristics depend on two parameters: (I) the ratio between the explosive weight and the flyer plate weight ( $R$  ratio), (II) the distance ( $X$ ) from the detonation point. The wavelength and amplitude of the modulation is an increasing function of both  $R$  and  $X$ . For values of  $R$ -ratio less than 1.4 the bonded interface is planar near the detonation point. The interface turns

to be wavy starting from a distance  $X$ , which is larger for smaller  $R$ -ratios. Increasing the  $R$ -ratio above  $R = 1.47$  results in a creation of a wavy interface starting close to the detonation point.

In a comparable study of a Cu–Fe casting it is found that first to solidify is the  $\gamma$ -Fe phase. As the temperature decreases after solidification the  $\gamma$ -phase transforms into the  $\alpha$ -Fe phase followed by copper precipitation.

The microstructure of the molten pockets seems to depend on both the cooling rate and the composition. Increasing either the cooling rate or the copper content results in finer microstructure. The similarity between the microstructure of molten pockets and the rapidly resolidified molten surfaces melted via high directed energy sources, suggests, that cooling rates as high as  $10^5 \text{ K sec}^{-1}$  are involved during molten pockets resolidification.

The bonding tensile strength is at least as high as the copper plate tensile strength. Usually the ruptured surface passes through the copper plate and not through the bonded interface.

#### Acknowledgement

The authors wish to thank Mr C. Cotler, Z. Vander and Z. Barkai for their technical aid and Dr Z. Burshtein for his editing remarks.

#### References

1. B. CROSSLAND and J. D. WILLIAMS, *Met. Rev.* **15** (1970) 79.
2. B. CROSSLAND, *Met. Mater.* **5** (1971) 401.
3. A. S. BAHRANI, T. J. BLACK and B. CROSSLAND, *Proc. Roy. Soc. A* **296** (1967) 123.
4. W. LUCAS, *J. Inst. Metals* **99** (1971) 335.
5. S. KOU, S. C. HSU and R. MEHRABIAN, *Met. Trans.* **12B** (1981) 33.
6. R. MEHRABIAN, *Int. Metals Rev.* **27** (1982) 185.
7. Y. CHUANG, R. SCHMID and Y. A. CHANG, *Met. Trans* **12A** (1984) 1921.
8. Z. LIVNE, "Structure phenomena in the bond zone of explosively bonded plates", Nuclear Research Center-Negev, NRCN 464 (1979).
9. L. F. TRUEB, *Trans. Met. Soc. AIME* **242** (1968) 1057.

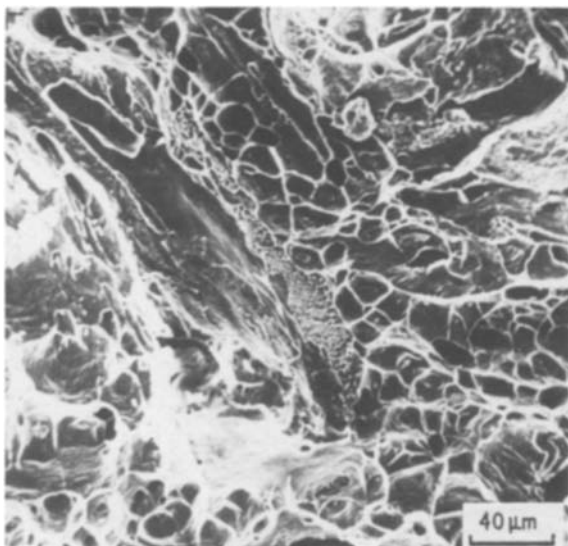


Figure 11 Secondary electron image showing a typical dimple structure of a ruptured Fe/Cu interface zone.

Received 9 June  
and accepted 18 August 1986